

## Correlation between rheological parameters and some colloidal properties of anatase dispersions

A.I. Gómez-Merino, F. J. Rubio-Hernández,  
J.F. Velázquez-Navarro, F.J. Galindo-Rosales, P. Fortes-Quesada  
Rheology and Electrokinetics Group, University of Málaga, Spain

### ABSTRACT

The linear relationship of the yield stress with the square zeta potential may be used to determine the Hamaker constant in solid dispersions. In this work we have obtained the Hamaker constant for the attractive force between anatase aqueous suspensions using this method and compared with those obtained by other techniques.

### INTRODUCTION

The van der Waals (attractive) and electrostatic (repulsive) forces play a critical role in determining the stability of dispersions. They form the basis of the well-known DLVO theory for colloid stability<sup>1,2</sup>. Depending on the stability level, differences in properties such as viscosity, flow and sedimentation behaviour in colloidal dispersions can be observed. For example, the viscosity of a flocculated dispersion can be several orders of magnitude larger than that for a dispersed dispersion at the same solid concentration<sup>3</sup>. Considering the role played in the stability of dispersions, it is suggested the necessity to characterize the van der Waals interaction between colloidal particles.

The value of the van der Waals force for pair interaction is greatly determined by the Hamaker constant. This parameter is material dependent and cannot be directly measured. Its theoretical value can be calculated from Lifshitz's theory<sup>4,5</sup>. This calculation requires that some dielectric or optical properties of the material be known at a wide frequency

spectrum. As these full spectra data are difficult to obtain for most materials, a number of approximate models, derived from Lifshitz's theory, that use a limited frequency data were developed<sup>6,7</sup>. The theoretical value of the Hamaker constant corresponding to some materials agrees with the experimental, however, in other cases, the disagreement was as high as a factor of seven.

Surface force apparatus (SFA)<sup>8,9</sup> and atomic force microscope (AFM)<sup>10</sup> are sophisticated experimental techniques that can be used to determine the Hamaker constant from DLVO theory. However, the results are very sensitive to the presence of impurities. Alternatively, the yield stress-zeta potential technique here used works with concentrated dispersions and, consequently, the results obtained are less sensitive to the relative smaller amount of impurities introduced from external sources. When flocculated, the particles in the colloidal dispersion are linked together by a net attractive force. These form a 3-D network that occupies the whole volume of the dispersion. The magnitude of the net attractive force determines the strength of the structure. The yield stress is a direct measure of the strength of this structure<sup>3,11,12</sup> and gets its maximum value at the isoelectric point (IEP). The IEP is the pH value corresponding to zero repulsive interaction, therefore only the van der Waals force contributes to strength of the structure<sup>3,11,12</sup>. If the pH is different from the IEP, the yield stress should decrease as the particles develop a larger repulsive potential.

Eventually, at a certain pH, the yield stress becomes zero. The surface potential (zeta potential) on the particles at this pH-value, characterizes the transition from a flocculated to a wholly dispersed state<sup>13,14</sup>. This critical zeta potential characterises the electrostatic repulsive potential that exactly counters the van der Waals attractive potential. Therefore, the critical zeta potential can be used to calculate the Hamaker constant.

In this paper we will measure the flow behaviour of anatase concentrated dispersions to determine the Hamaker constant of TiO<sub>2</sub> particles in water. For this purpose, a combined yield stress-zeta potential technique has been used.

#### THEORETICAL BACKGROUND

As it is well established in Electrokinetics, the zeta potential, measured at a shear plane near the surface particle, can be used as a good approximation to the surface potential, mainly when no specific adsorption takes place on the particles. The zeta potential is greatly dependent of the ionic strength at the liquid phase. At high ionic strength, the potential decreases much more sharply over the distance from the surface to the shear plane. This means a smaller zeta potential. It is therefore important to maintain a relatively constant ionic strength while characterizing the zeta potential of dispersion as a function of pH.

A linear relationship between yield stress and the square zeta potential has been validated by many aqueous dispersions<sup>13,14,15,16</sup>. By assuming that the yield stress is proportional to the particle pair DLVO interaction potential (or force), Hunter and Hunter et al. obtained an equation that predicts such a linear relationship. The yield stress of a particle network structure in a flocculated dispersion is proportional to the number of particle-particle links that cross a unit area of the sample and the strength of the links between particles. The relationship between yield stress ( $\tau_y$ ) and zeta potential ( $\zeta$ ) is given by<sup>17</sup>,

$$\tau_y = \frac{\phi^2}{a} \left( \frac{A}{12D_0^2} - \frac{C}{D_0} \zeta^2 \right) \quad (1)$$

where  $A$  is the Hamaker constant of the particle in water,  $C = 2\pi\epsilon \ln \left[ 1/(1 - e^{-\kappa D_0}) \right]$ ,  $D_0$  is the minimum surface separation distance between interacting particles in the flocculated state,  $\epsilon$  is the permittivity of water,  $\kappa$  is the inverse of the double-layer thickness which surrounds the colloidal particle,  $a$  is the particle size and  $\phi$  is the solid volume fraction of the dispersion. At the flocculated-dispersed state transition, the yield stress is zero. Essentially, at this state, the electrostatic repulsive potential is equal to the van der Waals attractive potential. The critical zeta potential  $\zeta_{crit}$  characterizing this transition is therefore given by,

$$\zeta_{crit} = \sqrt{\frac{A}{12D_0C}} \quad (2)$$

As can be seen, for a constant ionic strength, the critical zeta potential is proportional to the square root of Hamaker constant. According with Eq. 2, the critical zeta potential should not be dependent upon the particle size, size particle distribution, and solid concentration. Zhou et al.<sup>18</sup> confirmed this fact with a study on  $\alpha$ -Al<sub>2</sub>O<sub>3</sub> dispersions.

#### MATERIALS AND METHODS

The titanium oxide (TiO<sub>2</sub>), supplied by Sigma Aldrich, has a purity of 99.9 %, and a density of 3.9 g/cm<sup>3</sup>, a BET area of 10 m<sup>2</sup>/g, and an average primary particle size (TEM) of 100 nm.

The water was double distilled and deionised with a column of mixed bed ions (Millipore). All chemicals were of analytical grade. All measurements were performed at 25.0±0.1 °C.

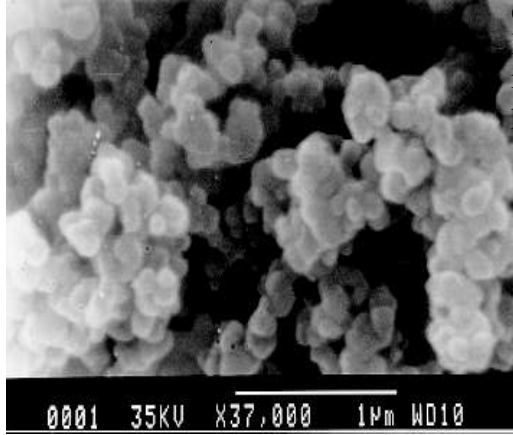


Fig. 1. Particle morphology of the TiO<sub>2</sub> nanoparticles used in the study.

concentration and can be characterised by the Debye length,  $\kappa^{-1}$ , which characterises the range of the electrostatic repulsion between particles.

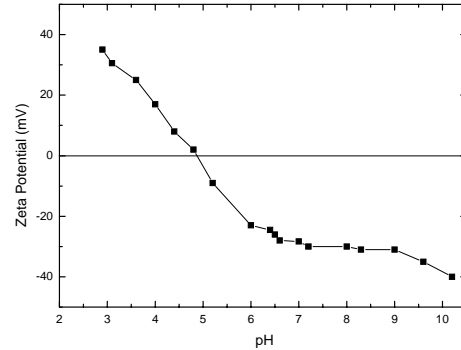


Fig. 2. The effect of pH on the zeta potential of anataze TiO<sub>2</sub> dispersions, for 10<sup>-5</sup> M KCl.

The dispersions were prepared by sonication the powder in water that was previously acidified with HCl or made alkaline with NaOH. Concentrated HCl or NaOH solutions 1 M were used to change the dispersions pH so as to minimize dilution.

The zeta potential was calculated from electrophoretic mobility measurements, which were made with a Zetasizer 2000 (Malvern Instruments). A fixed solid concentration of 4·10<sup>-4</sup> g/mL was used in all electrophoresis measurements. At least six measurements were taken at the stationary level in a rectangular cell. The pHmeter used was calibrated with buffer solutions of pH 4.0 and 7.0.

The rheological measurements were made using a strain-controlled Bohling-Vor rheometer with a cone-plate geometry (1° and 40 mm diameter). Dispersions containing 10 or 25 vol. % solids were used. The contact angle was measured using a CAM 200 Optical Angle Meter.

The zeta potential for TiO<sub>2</sub> suspensions was measured as a function of pH at various levels of ionic strength and the results are shown in Fig. 2. Since adjustment of pH with acid or base will lead to the change in the ionic concentration of each suspension, the ionic strength was controlled by adding an appropriate amount of salt (KCl) after each

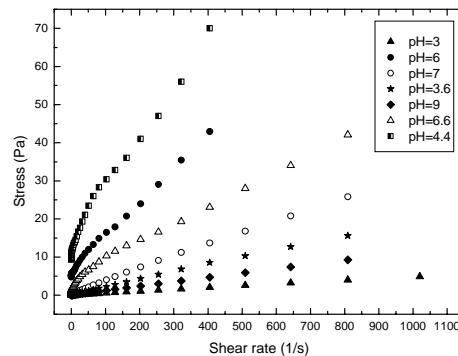


Figure 3. Flow curves for anataze TiO<sub>2</sub> dispersion as a function of pH,  $\phi = 0.25$ , for 10<sup>-5</sup> M KCl.

## RESULTS AND DISCUSSION

For the metal oxide dispersions, the magnitude of electrical double layer repulsive force is dependent on the surface charge density and the thickness of the double layer. The former is determined by the suspension pH. The latter is determined by the electrolyte

adjustment of pH to ensure the total ionic concentration coming from the salt and acid or base is nearly constant. The value for the IEP, pH=4.7, occurs at a lower pH than those given by other authors<sup>14,18</sup>. This can be due to the trace quantities of rutile found in this sample.

At pH near IEP, the effect of conductivity on zeta potential was not pronounced probably because the change in zeta potential with pH is quite sharp in this region. At pH further away from IEP, the effect of ionic strength is quite discernable for TiO<sub>2</sub>. The zeta potential is usually slightly higher for the lower ionic strength dispersion. But above IEP, the magnitude of the zeta potential is higher at lower ionic strength. The zeta potential attained a limiting value at pH well away from IEP. For TiO<sub>2</sub>, the limiting value at low pH is about 40 mV and, at high pH, it was about -48 mV at ionic strength between 10<sup>-3</sup> M and 10<sup>-5</sup> M of indifferent electrolyte.

Figures 3 and 4 show the flow curves for TiO<sub>2</sub> suspensions of  $\phi = 0.25$  and  $\phi = 0.10$  at different pH-values but a constant ionic strength. In both cases, the dispersions exhibited a shear-thinning flow behaviour over the shear rate range examined, which revealed that the particle aggregates in the suspensions were broken down into smaller flow units by the applied forces, so that the resistance to flow was reduced, leading to the lower viscosity as the shear rate increased. The

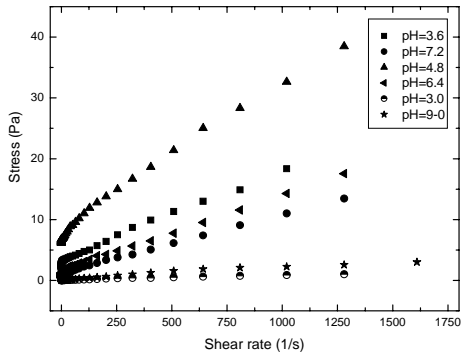


Figure 4. Flow curves for anatase TiO<sub>2</sub> dispersion as a function of pH,  $\phi = 0.10$ , for 10<sup>-5</sup> M KCl.

suspension began to flow so long as the applied stress was higher than the yield stress ( $\tau_y$ ). Various empirical models<sup>19</sup> were used to estimate  $\tau_y$ :

$$\text{Bingham plastic model: } \tau = \tau_{y,b} + \eta_s \dot{\gamma} \quad (3)$$

$$\text{Casson model: } \tau^{1/2} = \tau_{y,c}^{1/2} + (\eta_s \dot{\gamma})^{1/2} \quad (4)$$

$$\text{Herschel-Bulkley model: } \tau = \tau_{y,h} + K \dot{\gamma}^n \quad (5)$$

where  $\tau_{y,b}$ ,  $\tau_{y,c}$  and  $\tau_{y,h}$  are the yield-stress parameters determined from Bingham, Casson and Herschel-Bulkley models, respectively;  $\eta_s$  is the plastic viscosity, and K and n are structure-dependent parameters that can be determined experimentally. As can be expected, the yield stress,  $\tau_y$  increases with  $\phi$ , regardless of the model used. The Bingham plastic model supplies the highest yield stress comparing with the other models examined. This is presumably due to the linear  $\tau$ - $\dot{\gamma}$  dependence in Eq. 3.

The yield stress for each pH was calculated from Eqs. 3, 4 and 5. The criterion followed to choose the yield stress value was established on the basis of the most accurate adjustment obtained according to the fit parameters. The yield stress vs. pH data for TiO<sub>2</sub> dispersions is shown in figure 5. As can be seen, the maximum shear yield stress for each volume fraction concentration matches well with the isoelectric point. As the pH moves away from the IEP for both volume fractions, the shear yield stress decreases as the net attractive force decreases due to the increase in the electric double layer force as a result of the increase of surface charge density. When this repulsive force exceeds the van der Waals attraction at the pH far away from the IEP, dispersed suspensions are generated and the yield stress disappears.

The dispersion at  $\Phi=0.25$  is prepared in a dispersed state at a native pH=7.2. This dispersion displays a yield stress of 0.14 Pa. The pH of the dispersion is lowered in a stepwise manner. With a further reduction in the pH the yield stress increases and reaches a maximum value of 10.5 Pa at pH=4, however, a reduction in pH causes a decrease in the yield stress which eventually disappears at

pH=3. A similar behaviour was observed when the pH increases from the IEP.

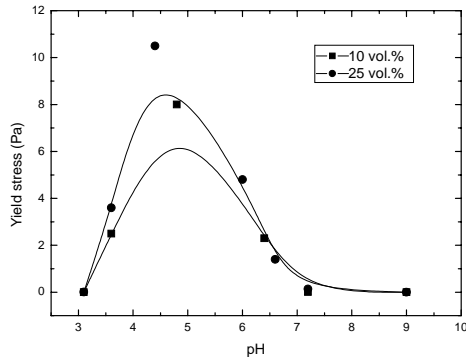


Figure 5. The yield stress of anatase TiO<sub>2</sub> dispersion as a function of pH.

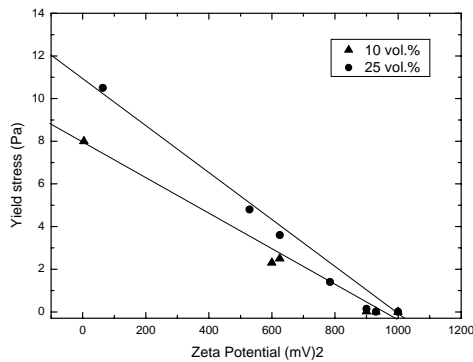


Figure 6. Yield stress vs. square of zeta potential for anatase TiO<sub>2</sub> dispersion at two volume fractions.

Thus, at pH=6, the value obtained for the yield stress is 4,8 Pa, and at pH=9, when the experiment is terminated, a small change in the yield stress is observed from the value found at the native pH. The same tendency described above is also observed in the case of  $\Phi=0.10$ . For this volume fraction the maximum yield stress attained is 8.0 Pa at pH=4.4. Further reduction of pH causes a decrease in the yield stress until the very small value 0.002 Pa at pH=3. Far away from the

IEP, at pH=9 the yield stress almost disappears, as could be expected. Not surprisingly, the maximum yield stress  $\tau_{y,max}$  exhibited a concentration dependence.

At the IEP, the yield stress is maximum because the electrostatic repulsive potential is absent. The linear relationship between yield stress and square of zeta potential  $\zeta^2$  for TiO<sub>2</sub> dispersions is shown in figure 6. The critical zeta potential is determined from the intercept on the  $\zeta^2$  axis. The critical zeta potential was 33 mV for  $\Phi=0.25$  and 31 mV for  $\Phi=0.10$ . The difference in the critical zeta potential of only 2 mV may not be experimentally significant. Although the ionic strength was not monitored during the yield stress measurement,  $10^{-5}$  M KCl is added to the dispersions as background electrolyte.

Other authors<sup>18,20</sup> have recently reported yield stress vs. zeta potential data for oxides suspensions at different concentrations and with different particles sizes. However, the ionic strength in these dispersions was not monitored during the yield stress measurement, but 0.01 M KNO<sub>3</sub> was added to the dispersions as background electrolyte. The critical zeta potential obtained from these data was found to be not dependent upon solids concentration and particle size. Leong et al.<sup>14</sup>, have also reported data of yield stress vs square of zeta potential for anatase TiO<sub>2</sub> and  $\gamma$ -Al<sub>2</sub>O<sub>3</sub> dispersions, and the critical zeta potential determined using this method was not significantly affected by the solid concentration.

From Eq. 2 the critical zeta potential is proportional to the square root of the Hamaker constant. The mean value obtained for anatase suspensions according with the data shown in figure 5 was  $44 \times 10^{-21}$  J. We have also estimated the Hamaker constant through the contact angle measurements, and the value obtained is  $34.85 \times 10^{-21}$  J. Both values are in good agreement with those reported by other authors<sup>21</sup>. The large discrepancy in the Hamaker constant data in the literature clearly reflects the imprecise and inaccurate nature of the current techniques or methods for determining the Hamaker constant of solids.

With this new zeta potential yield stress technique, the precision for Hamaker constant determination may be improved.

## CONCLUSIONS

The relationship between yield stress and the square of zeta potential is linear with a negative slope for TiO<sub>2</sub> dispersions, indicating that the suspension behaviour obeys the DLVO theory. A critical zeta potential of 32 mV has been obtained for TiO<sub>2</sub> suspensions, at an ionic strength of 10<sup>-5</sup> M KCl.

From the critical zeta potential, the estimated Hamaker constant is 37x10<sup>-21</sup> J, which is in good agreement with the experimental value obtained by the contact angle technique of 34.85 x10<sup>-21</sup> J.

The yield stress-zeta potential technique can be used as an indirect measure of the Hamaker constant, and it is capable of characterising dispersions with solid concentration as high as that used in the yield stress measurement, and the results obtained are usually insensitive to the relatively small amount of impurities. This technique can also be used as an indirect measure of the strength of the attractive interaction between particles in dispersions in the flocculated state.

## ACKNOWLEDGMENTS

A.I.G.M. would like to acknowledge the Group of Rheology of the Twente University (The Netherlands), in which part of this work was carried out, and the University of Málaga for the financial support.

## REFERENCES

1. Dejarguin B.V., Landau, L. (1941) *Acta Phys. Chim. URSS*, **14**, 633.
2. Verwey, E.J.W., Overbeek, J.Th.G. (1948), "*Theory of the Stability of Lyophobic Colloid*", Elsevier, Amsterdam.
3. Leong, Y.K., Boger, D.V., Parris, D. (1991), *J. Rheol.*, **35**, 149.
4. Lifshitz, E.M. (1956), *Sov. Phys. JETP* **2**, 73.
5. Dzyaloshinskii, I.E.; Lifshitz, E.M., Pitaevskii, L.P. (1961), *Ad. Phys.*, **10**, 165.

6. Tabor, D., Winterton, R.H.S. (1969), "*Proc. R. Soc. London.*", A 312, 435.
7. Hough, D.B., White, L.R. (1980), *Ad. Colloid Interface Science*, **14**, 41.
8. Israelachvili, J.N., Adams, G.E. (1978), *J. Chem. Soc., Faraday Trans.*, **74**, 975.
9. Luckham, P.F. (1989), *Powder Tecnology*, **58**, 75.
10. Larson, I., Drummond, C.J., Chan, D.Y.C., Grieser, F. (1993), *J. Am. Chem. Soc.*, **115**, 11885.
11. Leong, Y.K., Scales, P.J., Healy, T.W., Boger, D.V. (1995), *J. Am. Chem. Soc.*, **78**, 2209.
12. Leong, Y.K., Scales, P.J., Healy, T.W., Boger, D.V., Buscall, R. (1993), *J. Chem. Soc. Faraday Trans.*, **89**, 2473.
13. Leong, Y.K. (2000), Chemeca "2000, Perth, CD Proceedings", 314-319, ISBN 0-646-39910-1.
14. Leong, Y.K., Ong, B.C. (2003), *Powder Technology*, **134**, 249.
15. Hunter, R.J., Matarese, R., Napper, D.H. (1983), *Colloids Surf.*, **7**, 1.
16. Avramidis, K.S., Turian, R.M. (1991), *J. Colloid Interface Sci.*, **143**, 54.
17. Larson, R.G. (1999), "The Structure and Rheology of Complex Fluids", Oxford Univ. Press, New York.
18. Zhou, Z.W., Scales, P.J., Boger, D.V. (2001), *Chem. Eng. Sci.*, **56**, 2901.
19. Reed, J.S. (1995), "Principles of Ceramics Processing". Wiley, New York, USA.
20. Scales, P.J., Kapur, P.C., Johnson, S.B., Healy, T.W. (1998), "*A.I.Ch.E. Journal*", **44**, 538.
21. Ackler, H.D., French, R.H., Chaing, Y.M. (1996), *J. Colloid Interface Sci.*, **179**, 460.